Artificial Periodic Orbits Around L_1-Type Equilibrium Points for a Generalized Sail

Generoso Aliasi[*] Giovanni Mengali[†] and Alessandro A. Quarta[‡]

Department of Civil and Industrial Engineering, University of Pisa, I-56122 Pisa, Italy

Introduction

In recent years, many studies have been dedicated to the concept of displacing the five classical Lagrangian points of the Circular Restricted Three-Body Problem (CR3BP) [1, 2], using the propulsive acceleration of a spacecraft with a continuous-thrust propulsion system. To that end, the vehicle's thrust must be sufficient for balancing both the gravitational pull of the two massive bodies and the centrifugal force at a given point of the interplanetary space. When this happens, new families of Artificial Equilibrium Points (AEPs) may be generated and their main properties, in terms of location and stability, may be investigated. The most commonly proposed propulsion system for creating AEPs is the photonic solar sail [3], but examples exist in which the AEPs are generated using an electric thruster [4] or an electric solar wind sail (E-sail) [5].

The possibility of displacing an equilibrium position in the CR3BP is the starting point to investigate the existence of Artificial Periodic Orbits (APOs) around AEPs. For example, the use of collinear L_1-type AEPs for a scientific mission requires the spacecraft to be placed into an orbit with a suitable out-of-axis amplitude to drive the vehicle outside the so called "solar exclusion zone", thus avoiding problems of solar interference with down-link telemetry [6]. The use of an AEP with 5 deg offset from the Sun-[Earth+Moon] line is a possible choice [3], provided that a suitable attitude control strategy is employed to offset the thrust direction. Even though the characteristics of periodic orbits have been thoroughly studied around the collinear classical Lagrangian points [7], the properties of APOs have been investigated by a few authors only. In most cases the results have been obtained using a solar sail based

[*]Research Assistant, g.aliasi@dia.unipi.it

[†]Professor, g.mengali@ing.unipi.it. Senior Member AIAA.

[‡]Associate Professor, a.quarta@ing.unipi.it. Associate Fellow AIAA.

spacecraft. Examples of APOs generated by a solar sail are found in [8–10]. The capability of an electric thruster to generate APOs is analyzed in [11].

The contribution of this Note is to extend the available results for APOs maintained by a propellantless propulsion system to the case of purely radial (continuous) propulsive acceleration, whose modulus depends on a given power of the Sun-spacecraft distance. The assumption of radial thrust is particularly interesting as it can be representative of a situation in which the spacecraft attitude is maintained in a passive way. Moreover, a radial thrust implies that the problem is Hamiltonian, and there exists a first integral of motion (i.e. the total energy) that simplifies the numerical analysis. The concept of such an idealized thruster, referred to as generalized sail [12], unifies different continuous-thrust propulsion systems such as solar sails, E-sails [13], or electric thrusters.

Artificial Equilibrium Points

Consider a massless spacecraft, equipped with a continuous-thrust propulsion system, under the gravitational effect of both the Sun and the Earth+Moon system, and assume that the planet's orbit around the star is circular with radius $l \triangleq 1\,\mathrm{au}$. The spacecraft motion is described using a synodic reference frame $\mathcal{T}(C; x, y, z)$, with origin at the center-of-mass of the Sun-[Earth+Moon] system, which rotates synchronously to the revolution of the planet around the massive body. The x-axis points along the Sun-Earth line, the z-axis is in the direction of Earth+Moon's angular momentum, and y-axis completes the right-handed coordinate system.

The spacecraft propulsion system is modeled using the concept of a generalized sail [12], which is useful for describing the propulsive acceleration when the thrust is aligned along the Sun-spacecraft (radial) direction. The propulsive acceleration modulus varies with the Sun-spacecraft distance $l\rho_\odot$ proportional to $\beta/\rho_\odot^\eta$, where $\rho_\odot$ is the dimensionless Sun-spacecraft distance, the exponent $\eta \geq 0$ defines the propulsion system type and β, referred to as the lightness number, is a performance parameter that quantifies the spacecraft thrusting capabilities. The propulsive acceleration vector $\boldsymbol{a}_P$ provided by a generalized sail is [12]

$$\boldsymbol{a}_P = \beta \, \frac{G\, m_\odot}{l^2\, \rho_\odot^{\eta+1}} \, \boldsymbol{\rho}_\odot \tag{1}$$

where $Gm_\odot$ is the Sun's gravitational parameter and $\boldsymbol{\rho}_\odot$ is the dimensionless Sun-spacecraft vector.

A suitable choice of η allows the model to capture different types of propulsion systems [12], such as a solar sail ($\eta = 2$), an E-sail ($\eta = 1$), or a classical electric thruster. In the latter case, $\eta = 0$ if the thrust is modulated such as to provide a constant thrust-to-mass ratio and $\eta \approx 1.6$ for a solar electric thruster, i.e. when the electric power is supplied by solar arrays. Even though Eq. (1) could theoretically be used for any value of β and η, some constraints must be introduced to their range of variation to confine the succeeding analysis to currently available or near-future propulsion systems only. To that end it is assumed that $\beta \geq 0$ and $\eta \leq 2$, thus implying that the propulsive acceleration is outward directed from the Sun and decreases as the Sun-spacecraft distance is increased.

For a given parameter η, the value of β_0 required to meet the artificial equilibrium conditions (subscript "0") for L_1-type AEPs at a dimensionless distance $\rho_{\odot_0} = [(x/l)_0 + \mu] < 1$ from the Sun [12], is

$$\beta_0 = \frac{\mu\,\rho_{\odot_0}^{\eta}}{1-\mu}\left[1 - \frac{1}{\left(1-\rho_{\odot_0}\right)^2}\right] + \rho_{\odot_0}^{\eta-2} - \frac{\rho_{\odot_0}^{\eta+1}}{1-\mu} \tag{2}$$

where $\mu \approx 3.0359 \times 10^{-6}$ is the dimensionless mass of Earth+Moon.

Equation 2 shows that the classical L_1 Lagrangian point is recovered at $\rho_{\odot_{L_1}} \approx 0.989993$ when $\beta_0 = 0$. When $\eta \leq 2$, it can be verified that the L_1-type AEPs generated by a generalized sail are always in the form of saddle×center×center equilibrium solutions. Therefore, those AEPs are always unstable, and arbitrarily chosen initial positions and velocities generate unbounded spacecraft motions. However, with suitable initial conditions, the divergent mode related to the saddle dynamics may be suppressed and bounded spacecraft trajectories (the so-called Lissajous orbits) around the AEPs may be obtained [2]. In particular, as a consequence of Lyapunov's center theorem, families of periodic orbits may emanate from each of the AEP provided that the imaginary eigenvalues (referred to as $\pm j\omega_p$ and $\pm j\omega_z$) of a given AEP are not resonant, i.e. if their ratio is not an integer number.

Figure 1, which involves L_1-type AEPs in the Sun-[Earth+Moon] system, shows that resonance conditions exist for special values of β_0 only. In particular, for all η there exists a

value of β_0, referred to as β_D, such that a resonance condition 1:1 exists between ω_p and ω_z. Figure 1 shows the points corresponding to $\beta_D|_{\eta=0} \approx 0.07851$ and $\beta_D|_{\eta=1} \approx 0.09219$. Recall that when a resonance takes place, the Lyapunov's theorem does not guarantee the existence of any family of periodic orbits (therefore the values of β_D are important for the study of APOs). Also note that in the case $\eta = 2$, a 1:1 resonance exists as β_0 approaches one, i.e. in the limiting case when the solar sail propulsive acceleration equals the Sun gravitational acceleration and the AEP location coincides with the Sun's center-of-mass.

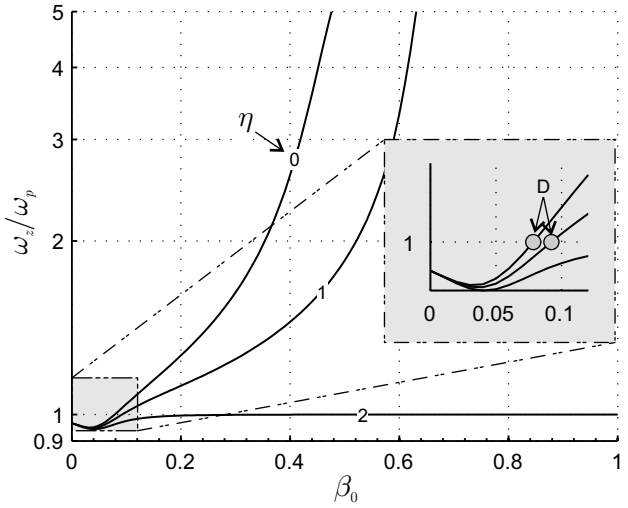

Figure 1: Imaginary eigenvalues ratio for L_1-type AEPs as function of $\beta_0 \in [0, 1]$ and $\eta \in \{0, 1, 2\}$.

Two families of periodic orbits generally arise from each AEP, which are referred to as Lyapunov planar and Lyapunov vertical orbits, respectively. Along these families, there may exist branching orbits, i.e. APOs that simultaneously belong to a different family. In particular, Lyapunov planar orbits and branching orbits originating from halo orbit families will now be investigated. Recall that halo orbits are three-dimensional periodic orbits symmetric with respect to the (x-z) plane.

Families of Artificial Periodic Orbits

Families of APOs have been obtained numerically with a Moore-Penrose continuation method. To this end, using the procedure described in [14], the spacecraft equation of motion has been reformulated as a boundary-value problem that was solved, at each step, using an

orthogonal collocation method. The values of β_0 considered in the simulations are consistent with present or near-future (generalized) sails. For example, the expected lightness number for the Sunjammer mission [15] is about 0.04, while a reference value for future β values is about 0.16.

Starting from the position of a given AEP, Lyapunov planar (LP) families of orbits have been generated for different values of β_0, while η is maintained fixed. Following the families obtained for a given value of β_0, branching points have been found that generate halo (H) orbits, referred to as LP-H, as they exist on the Lyapunov planar family. Finally, starting from the obtained branching points, some new families of halo orbits have been generated. Along the Lyapunov planar orbits, branching points have been found that generate axial orbits (referred to as LP-A branching points). Other families of periodic orbits may exist, possibly generated from other branching points, as for example the Lyapunov vertical, the backflip orbits and the axial orbits. A comprehensive catalog about possible CR3BP-periodic orbits is in [16].

The continuation algorithm is designed to stop continuation when a collision with Earth+Moon is detected, even though such an event could be overtaken either regularizing the equations of motion or continuing the orbits using the dimensionless mass μ as a parameter. Within this Note, a collision means that during the continuation process the spacecraft orbit touches a (virtual) sphere of radius 0.0027 au centered at the center-of-mass of Earth+Moon, roughly corresponding to Moon's apogee position. Such an event is marked with a white square (□) in Figs. 2 and 4. Black circles (●) and black lozenges (⧫) in Figs. 2 and 4 represent LP-H and LP-A branching points, respectively, while white circles (○) point out the AEPs position in the rotating reference frame.

The continuation algorithm also calculates the Floquet multipliers for each computed orbit, so that information on linear stability of orbits can be recovered. In particular, recall that the number of multipliers that are outside the unit circle gives the instability order of the orbit. Results involving particular values of η are now presented, which correspond to special propulsion systems, that is, electric thrusters ($\eta = 0$), E-sails ($\eta = 1$), and solar sails ($\eta = 2$).

Lyapunov Planar Orbits

Lyapunov planar families emanate from the AEP corresponding to the selected values of β_0 and η, and stop when a collision with Earth+Moon occurs, see Fig. 2. Each family presents two branching orbits, i.e. LP-H and LP-A, as long as $\beta_0 \leq \beta_D$. Typically, the y-amplitude of the branching points increases (solid lines joining LP-H or LP-A points in Fig. 2) up to a maximum value for $0 < \beta_0 < \beta_D$, beyond which the amplitude decreases (dotted lines in Fig. 2) to zero when $\beta_0 = \beta_D$. When $\beta_0 > \beta_D$, no branching points (neither LP-H nor LP-A) are found by the numerical algorithm, therefore neither halo nor axial orbits can be generated for values beyond β_D. Note that the numerical results obtained for $\eta = 2$ are consistent with the simulations of [9, 10].

Figure 2 also gives information about the linear stability of the computed orbits. In particular, trajectories that lie within the gray region of Fig. 2 correspond to order 2 instability orbits, whereas trajectories outside that region are unstable with an instability of order 1. For the case $\eta = 1$, Fig. 3 shows the shape of the periodic orbits for three different values of β_0: similar to the classical case ($\beta_0 = 0$), the Lyapunov planar orbits encircle the AEP from which they generate, and their amplitude increases until a collision is reached.

Halo Orbits

Halo orbit families emanate from the LP-H branching points along the Lyapunov planar families. For these families, there are four different behaviors depending on the value of β_0. For small values of β_0, the behavior of each family is similar to the classical case $\beta_0 = 0$, as the orbits continuously rise up from the (x-y) plane to terminate in a collision with Earth+Moon, see Fig. 4.

According to Fig. 4, while $\beta_0 < \beta_1^H$ is increased, halo families start to fold back until the value $\beta_0 = \beta_1^H$ is reached. At this point an orbit along the family becomes planar. As suggested in [9] for $\eta = 2$, this situation represents a new branching orbit that generates the so called Retrograde Satellite (RS) orbits. A second family of halo orbits, not calculated here, emanates from another branching orbit along the RS families [9]. This critical case indicates a change in the topology of the halo families, as for $\beta_1^H < \beta_0 < \beta_2^H$ the halo orbits stop when the planar orbit is reached, without folding back. Another change takes place

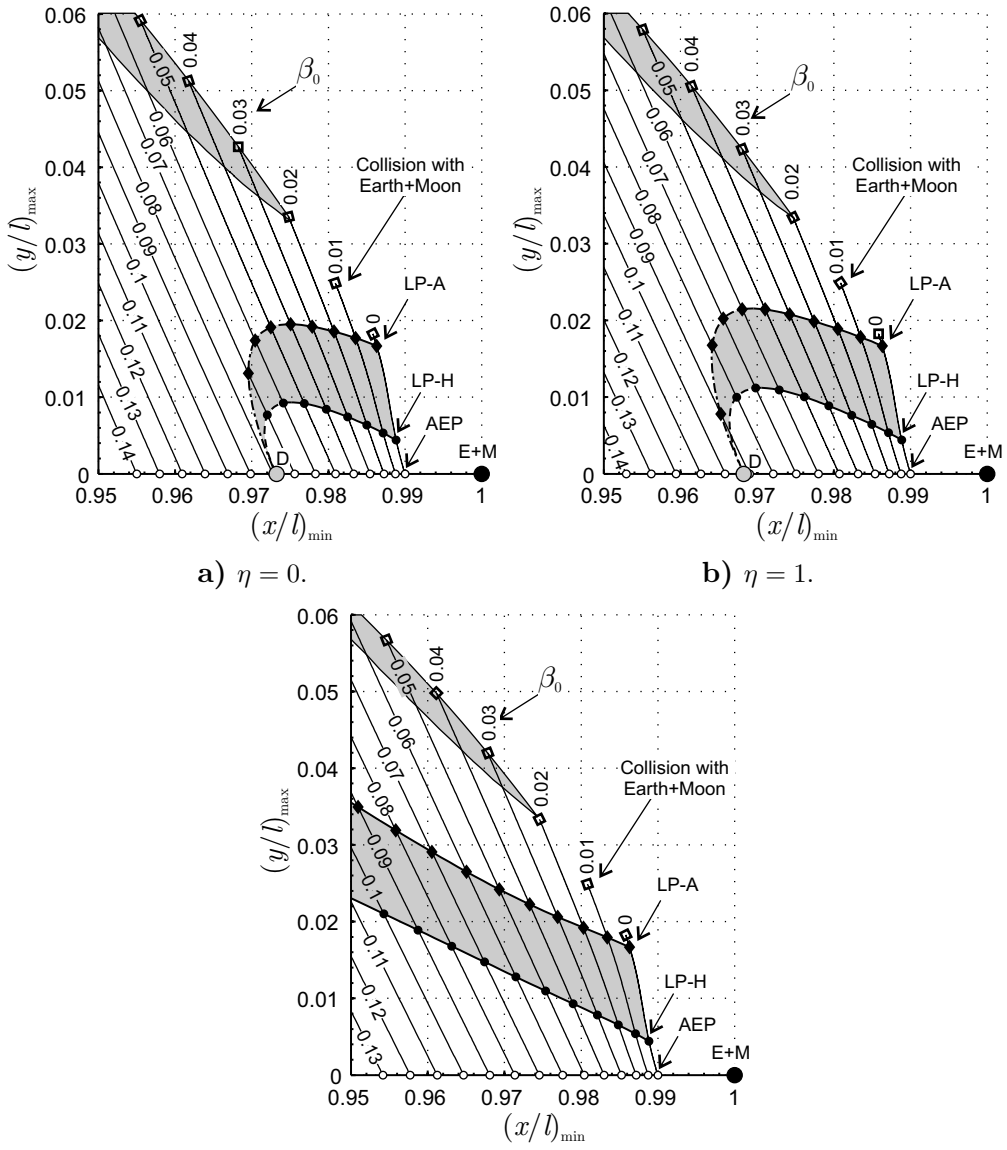

a) $\eta = 0$.

b) $\eta = 1$.

c) $\eta = 2$.

Figure 2: Families of Lyapunov planar orbits as function of $\eta \in \{0, 1, 2\}$ and $\beta_0 \in [0,\ 0.13]$ with a step variation of 0.01.

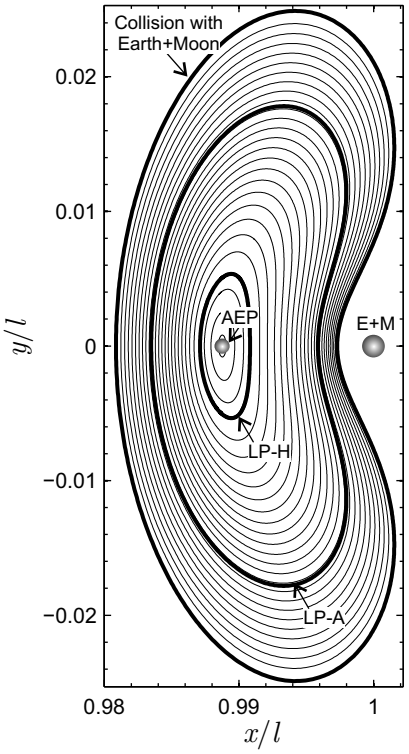

a) $\beta_0 = 0.01$.

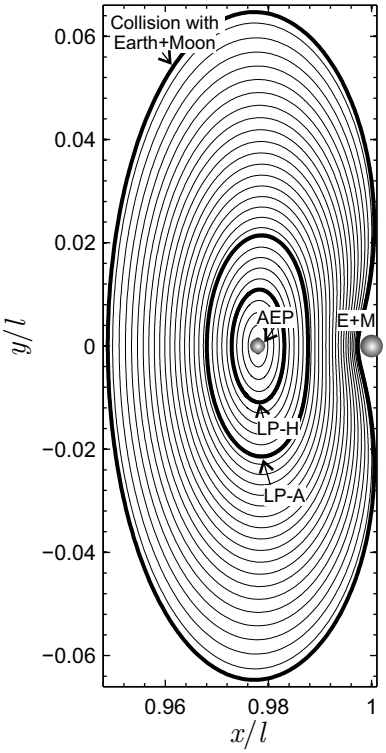

b) $\beta_0 = 0.06$.

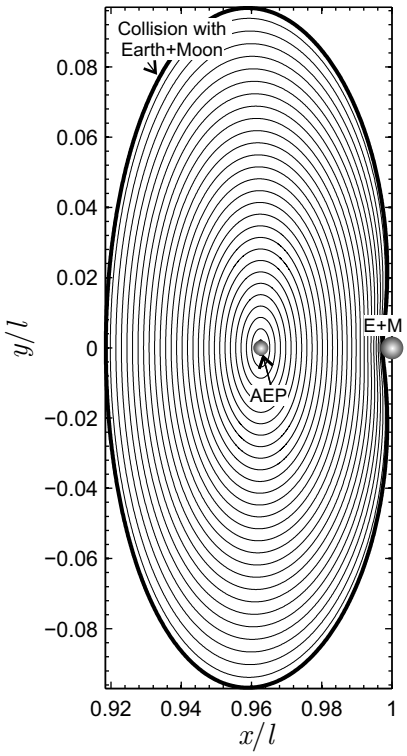

c) $\beta_0 = 0.11$.

Figure 3: Lyapunov planar orbits (about 30) as a function of $\beta_0 \in \{0.01, 0.06, 0.11\}$ with $\eta = 1$.

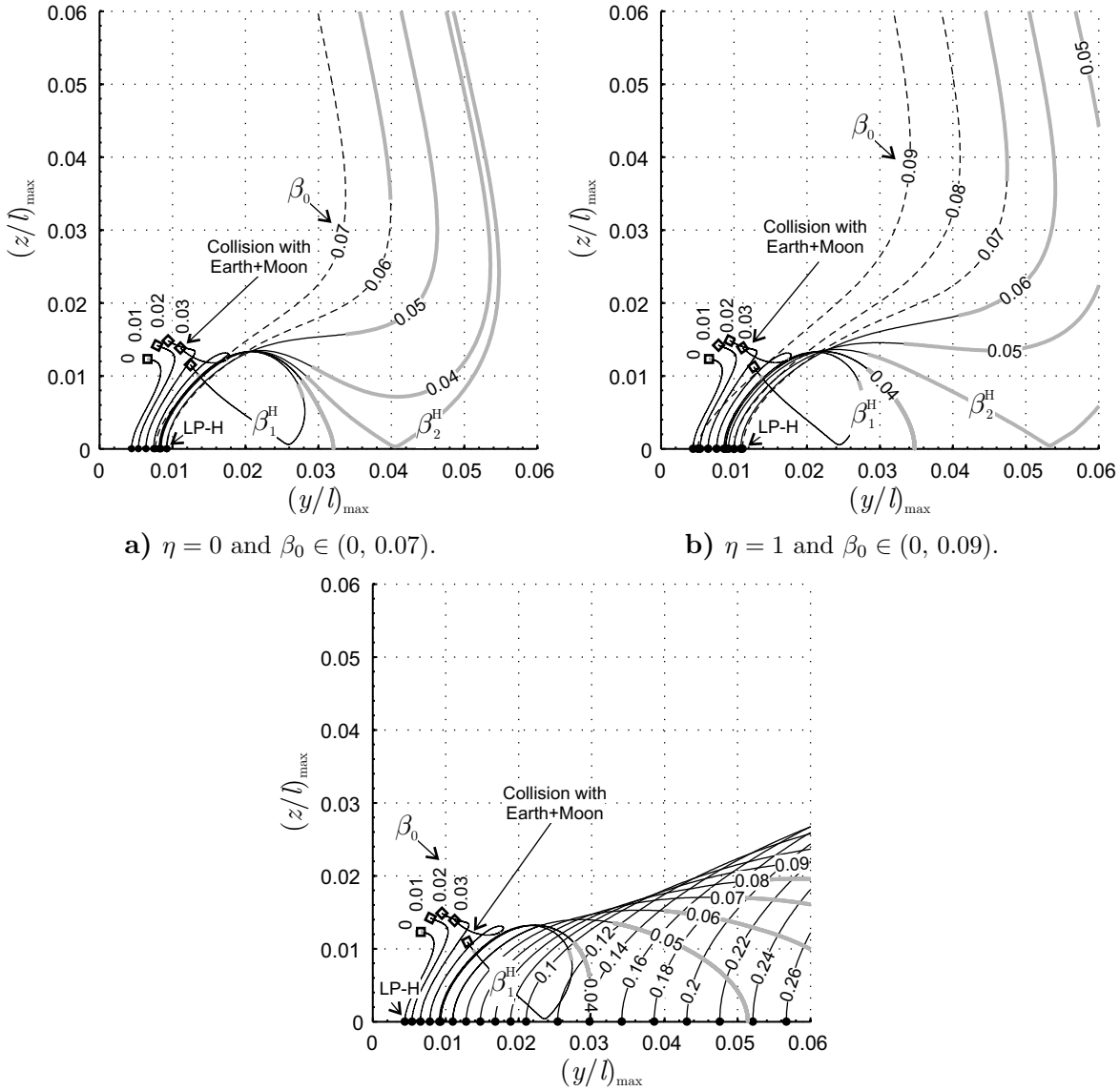

a) $\eta = 0$ and $\beta_0 \in (0,\, 0.07)$.

b) $\eta = 1$ and $\beta_0 \in (0,\, 0.09)$.

c) $\eta = 2$ and $\beta_0 \in (0,\, 0.26)$.

Figure 4: Families of halo orbits as a function of $\eta \in \{0, 1, 2\}$ and β_0.

when $\beta_0 = \beta_2^H$, at which the halo rises again when the planar orbits is reached. Finally, for $\beta_0 > \beta_2^H$ the families do not touch the (x-y) plane in the neighborhood of the AEPs, and raise to higher values of z-amplitude. For higher values of β_0, halo families are generated by branching points that lie beyond the maximum of the LP-H line of Fig. 2. These families are plotted as dashed lines in Fig. 4. Note that Fig. 4 also shows, using thick and gray lines, the orbits with order 0 instability (also called neutral stability), whereas the black lines correspond to unstable orbits of order 1 or 2. The critical values β_1^H and β_2^H depend on the propulsion system type, when the dimensionless mass μ is fixed. The values corresponding to the families drawn in Fig. 4 are summarized in Table 1 along with the value of β_D.

η	β_1^H	β_2^H	β_D
0	0.03759	0.03856	0.07851
1	0.03828	0.04329	0.09219
2	0.03890	0.2894	1

Table 1: Critical values of β_0 (β_2^H for $\eta = 2$ is taken from [9]).

Figure 5 shows the northern halo orbits for $\eta = 1$ with values of β_0 corresponding to the three different behaviors depicted in Fig. 4. Families start from the branching orbit (LP-A) along the Lyapunov planar families, and behave differently depending on the value of β_0. The southern orbits also exist for the same values of β_0. They can be obtained by simply mirroring each family with respect to the (x-y) plane, as in the classical problem.

Conclusions

Lyapunov planar orbits may be generated as a function of the spacecraft performance, except for some isolated points when a resonance occurs between the imaginary eigenvalues of the linearized motion around the equilibrium point. As for the halo families, the numerical simulations show that for each thruster type a critical value of the propulsive acceleration exists beyond which such orbits disappear. The critical value is associated to the existence of a 1:1 resonance between the imaginary eigenvalues. As far as halo orbits are concerned, two other critical values can be detected for each propulsion system type. These values correspond to a change in the way the families of artificial periodic orbits evolve. Simulations show that,

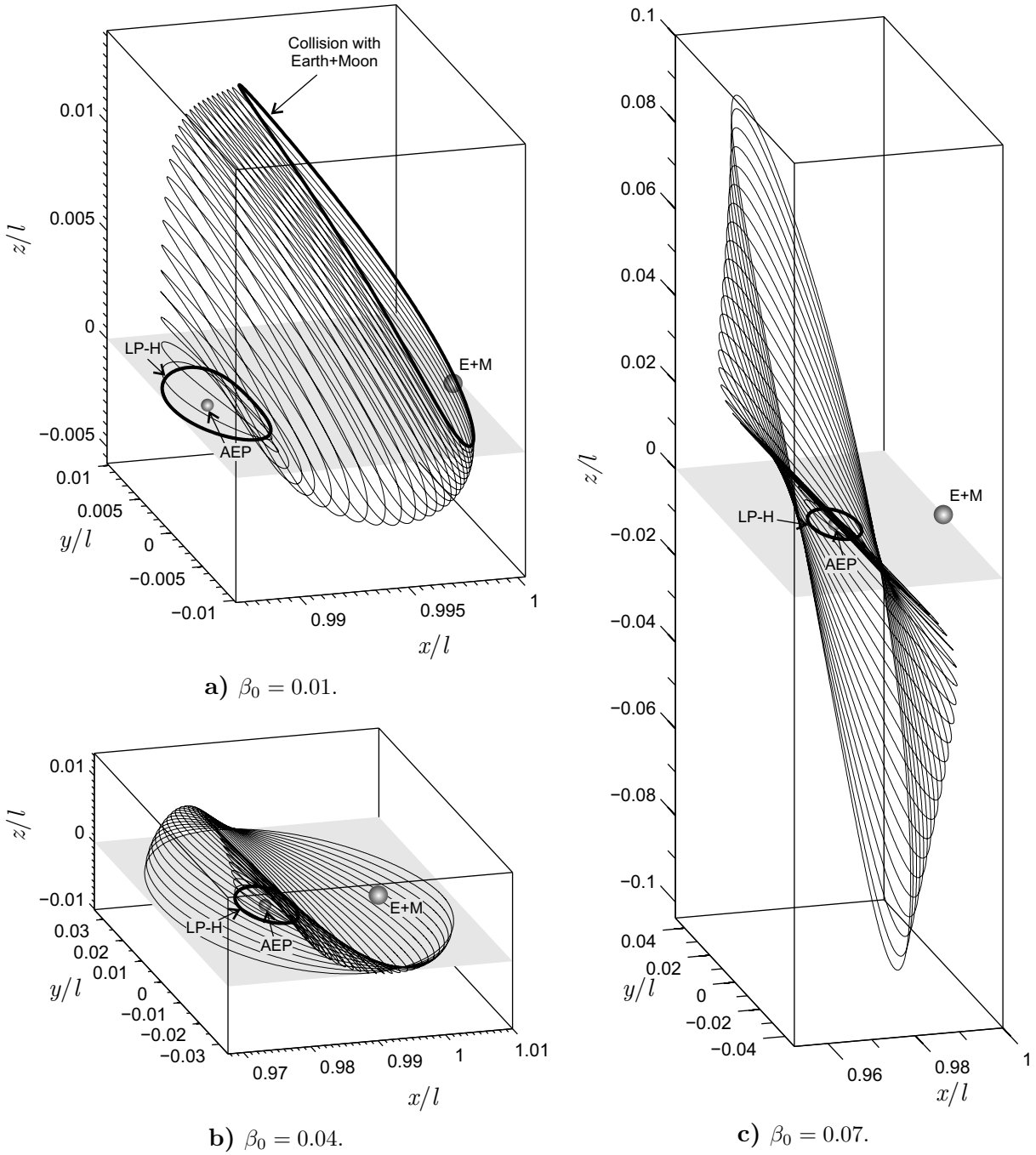

a) $\beta_0 = 0.01$.

b) $\beta_0 = 0.04$.

c) $\beta_0 = 0.07$.

Figure 5: Northern halo orbits for $\eta = 1$ (E-sail case).

for the same value of β_0, the size and shape of Lyapunov planar orbits are similar. On the contrary, Halo orbits are characterized by different sizes and shapes.

References

[1] Battin, R. H., *An Introduction to the mathematics and methods of Astrodynamics*, chap. 8, AIAA, New York, 1987, pp. 371–386, ISBN: 1-563-47342-9.

[2] Szebehely, V., *Theory of orbits: the restricted problem of three bodies*, chap. 4, 5, Academic Press, New York, 1967, pp. 126–318, ISBN: 0-126-80650-0.

[3] McInnes, C. R., McDonald, A. J. C., Simmons, J. F. L., and MacDonald, E. W., "Solar sail parking in restricted three-body systems," *Journal of Guidance, Control, and Dynamics*, Vol. 17, No. 2, March-April 1994, pp. 399–406. doi: 10.2514/3.21211.

[4] Morimoto, M., Yamakawa, H., and Uesugi, K., "Artificial equilibrium points in the low-thrust restricted three-body problem," *Journal of Guidance, Control and Dynamics*, Vol. 30, No. 5, September-October 2007, pp. 1563–1567. doi: 10.2514/1.26771.

[5] Aliasi, G., Mengali, G., and Quarta, A. A., "Artificial Equilibrium Points for Electric Sail with Constant Attitude," *Journal of Guidance, Control, and Dynamics*, Vol. 6, No. 50, November-December 2013, pp. 1295–1298. doi: 10.2514/1.A32540.

[6] Howell, K. C. and Pernicka, H. J., "Sun-Earth libration point trajectories that avoid the solar exclusion zone," *Journal of the Astronautical Sciences*, Vol. 38, No. 3, July-September 1990, pp. 269–288.

[7] Breakwell, J. V. and Brown, J. V., "The 'Halo' family of 3-dimensional periodic orbits in the Earth-Moon restricted 3-body problem," *Celestial Mechanics*, Vol. 20, No. 4, November 1979, pp. 389–404. doi: 10.1007/BF01230405.

[8] Ceriotti, M. and McInnes, C., "Natural and sail-displaced doubly-symmetric Lagrange point orbits for polar coverage," *Celestial Mechanics and Dynamical Astronomy*, Vol. 114, No. 1-2, October 2012, pp. 181–190. doi: 10.1007/s10569-012-9422-2.

[9] Verrier, P., Waters, T., and Sieber, J., "Families of Periodic Orbits for Solar Sails in the CRBTP," *Advances in Solar Sailing*, edited by M. Macdonald, Springer Praxis Books, Springer Berlin Heidelberg, 2014, pp. 871–884.

[10] Verrier, P., Waters, T., and Sieber, J., "Evolution of the L_1 Halo family in the radial solar sail CRTBP," *Celestial Mechanics and Dynamical Astronomy*, Vol. 120, No. 4, December 2014, pp. 373–400. doi: 10.1007/s10569-014-9575-2.

[11] Baig, S. and McInnes, C. R., "Artificial halo orbits for low-thrust propulsion spacecraft," *Celestial Mechanics and Dynamical Astronomy*, Vol. 104, No. 4, August 2009, pp. 321–335. doi: 10.1007/s10569-009-9215-4.

[12] Aliasi, G., Mengali, G., and Quarta, A. A., "Artificial Equilibrium Points for a Generalized Sail in a Circular Restricted Three-Body Problem," *Celestial Mechanics and Dynamical Astronomy*, Vol. 110, No. 4, August 2011, pp. 343–368. doi: 10.1007/s10569-011-9366-y.

[13] Janhunen, P. et al., "Electric solar wind sail: toward test missions," *Review of Scientific Instruments*, Vol. 81, No. 11, November 2010, pp. 111301–1–11301–11. doi: 10.1063/1.3514548.

[14] Govaerts, W., Kuznetsov, Y. A., De Witte, V., Dhooge, A., Meijer, H., Mestrom, W., Riet, A., and Sautois, B., *MATCONT and CL_MATCONT: Continuation toolboxes in Matlab*, `http://sourceforge.net/projects/matcont/files/Documentation/ManualSep2012.pdf/download`.

[15] Heiligers, J., Diedrich, B., Derbes, B., and McInnes, C., "Sunjammer : Preliminary end-to-end mission design," *AAS/AIAA Astrodynamics Specialist Conference*, San Diego, August 4–7, California 2014.

[16] Doedel, E. J., Romanov, V. A., Paffenroth, R. C., Keller, H. B., Dichmann, D. J., Galàn-Vioque, J., and Vanderbauwhede, A., "Elemental Periodic Orbits Associated with the Libration Points in the Circular Restricted 3-Body Problem," *International Journal of Bifurcation and Chaos*, Vol. 17, No. 8, August 2007, pp. 2625–2677. doi: 10.1142/S0218127407018671.